

Original Article

Analysis of ASER with QAM Techniques for SISO Communication Subject to α - μ Fading Channels

Rajkishur Mudoï

Department of Electronics and Communication Engineering, North-Eastern Hill University, Shillong, Meghalaya, India.

Corresponding Author : rajkishur@gmail.com

Received: 13 June 2023

Revised: 16 July 2023

Accepted: 12 August 2023

Published: 31 August 2023

Abstract - In α - μ fading environment utilizing Quadrature Amplitude Modulation (QAM) schemes, the Average Symbol Error Rate (ASER) is analyzed for a Single Input And Single Output (SISO) communication system. QAM schemes enhance bandwidth efficiency for 5G and beyond wireless transmission systems. The closed-form expressions for the ASER of Hexagonal QAM (HQAM), Cross QAM (XQAM), Square QAM (SQAM), as well as Rectangular QAM (RQAM) schemes are presented using Fox H-function, which is the most general function and Prony approximation for Gaussian Q-function is utilized. The α - μ distribution considers the nonlinearity of the propagation medium and the nonhomogeneous medium. Analytical results show tight agreement with simulation data.

Keywords - α - μ fading, ASER, Fox H-function, Quadrature Amplitude Modulation, Prony approximation.

1. Introduction

Quadrature Amplitude Modulation (QAM) is an outstanding modulation technique to improve the spectral efficiency Beyond Fifth-Generation (5G), and 6G radio broadcasting systems, Quadrature Amplitude Modulation (QAM) is an outstanding modulation technique. QAM applies both the amplitude and phase variations to use the bandwidth efficiently. Regarding data high-rate radio communication directions, different QAM schemes can be used. To achieve high data rates at low energy, Hexagonal QAM (HQAM) is employed. HQAM has more power efficient Two Dimensional (2D) hexagonal-shaped constellations, thereby reducing the peak and average power of the constellation [1] [2]. HQAM is commonly applied in advanced channel coding, optical communications, multicarrier and multiple-antenna systems [2].

Cross-QAM (XQAM) constellation has a cross shape, which can be found in a square constellation by deleting some outside points in each edge. The peak and average power can be decreased by employing the XQAM constellation, thereby increasing the average SNR. XQAM is used to transmit an odd number of bits per symbol. The applications of XQAM are obtained in Very high-speed Digital Subscribers Line (VDSL), Asymmetric Digital Subscribers Line (ADSL), as well as Digital Video Broadcasting-Cable (DVB-C) transmission for multimedia services [3],[10]. Square QAM (SQAM) is required for an even power of 2 QAM constellations. The odd power of 2 constellations like Rectangular QAM (RQAM) is chosen for

better channel adaptation and data rate. SQAM is commonly applied in Wireless Fidelity (Wi-Fi), satellite communications, and digital video broadcast [4].

RQAM is a common modulation technique because it covers Binary Phase Shift Keying (BPSK), SQAM, multilevel amplitude shift keying, orthogonal binary frequency shift keying, as well as Quadri Phase Shift Keying (QPSK) as particular cases. RQAM is deployed in high-speed cellular communication systems, telephone-line modems, asymmetric subscriber loops, and microwave communications [5], [6].

The Single-Input and Single-Output (SISO) is a typical model for mobile communication systems, where a single transmitting antenna is employed with the transmitter, and the receiver employs a single receiving antenna. The benefit of a SISO system is that it is effortless to model and realize, and the cost is also low. α - μ fading distribution represents the channel of the system. The α - μ fading model deals with a signal consisting of clusters of multipath waves passing through nonhomogeneous surroundings. The phases of the scattered waves internal to a cluster are random.

The scattered waves within the clusters of multipath waves have identical powers. The α - μ distribution is a standard fading distribution which consists of the Weibull, Gamma, Nakagami- m , exponential, Rayleigh, and one-sided Gaussian distribution for specific values of α as well as μ [7]. The ASER investigation of different QAM schemes given



fading environments has been stated in some articles. In [8], the expression of the average Symbol Error Probability (SEP) considering the XQAM scheme under independent but not necessarily identical (i.n.i.d) η - μ fading distribution is examined for Maximal-Ratio Combining (MRC) diversity receiver. The results are obtained concerning Lauricella hypergeometric functions. In [9], the ASER expressions of XQAM and RQAM schemes under a Two-Wave with Diffuse Power (TWDP) fading condition are analyzed.

The ASER expressions are obtained in connection with Appell's and Lauricella's hypergeometric functions utilizing the moment-generating function-based approach. In, the expressions of ASER applying RQAM and general-order HQAM techniques are presented for multiple amplify-and-forward relay-based communications under i.n.i.d Nakagami- m fading channels and applying a CDF-based method.

In [11], the SER performance of general order M -ary QAM is investigated subject to the effect of the Fisher-Snedecor F fading model. In [12], the ASER is investigated with different QAM techniques subject to the Alternate Rician Shadowed (ARS) fading environment. The ASER is presented utilizing the elementary functions and Meijer's G functions.

In [13], the SEP with HQAM scheme for a dual-input Selection Combining (SC) diversity receiver is investigated considering the links experienced with η - μ fading channels. In [14], the authors have presented a closed-form SEP approximation for the high-order HQAM constellations without considering the fading environments. [17] examines the SER performances with different QAM schemes for low-power backscatter communications.

Influenced by the functionality as well as importance, the ambition of this task is to carry out a numerical analysis for the action of the SISO communication [16] scheme considering the effect of an α - μ fading distribution under different QAM techniques. The following main improvements are performed in this work.

- A novel output SNR PDF derivation at the receiver of the SISO cellular transmission is presented in terms of Fox H -function.
- The important mathematical derivations of ASER for HQAM, XQAM, SQAM, and RQAM methods are derived in the presence of α - μ fading channels, and outcomes are illustrated.

2. Channel Model

The base station with a single transmitting antenna transmits the signal to the user deploying the QAM technique. The user has a single receiving antenna, constituting a SISO transmission system.

A - μ fading distribution influences the channel between the transmitter and receiver. The PDF of the fading amplitude H is yielded by [7],

$$f_H(h) = \frac{\alpha \mu^\mu h^{\alpha\mu-1}}{h^{\alpha\mu} \Gamma(\mu)} \exp\left(-\mu \frac{h^\alpha}{\alpha}\right) \quad (1)$$

Where the parameter α denotes the nonlinearity of the environment, and μ describes the number of multipath clusters. $\bar{h} = \alpha \sqrt{E(H^\alpha)}$ and $E(\cdot)$ denotes the expectation.

$\Gamma(\cdot)$ denotes the Gamma function. Let $W = |H|^2$ is the instantaneous channel power gain with unit mean. Applying RV transformation in (1), the PDF of w is written as

$$f_W(w) = \frac{\alpha \mu^{\frac{\alpha\mu-1}{2}}}{2\Omega^{\frac{\alpha\mu}{2}} \Gamma(\mu)} \exp\left[-\left(\frac{w}{\Omega}\right)^{\frac{\alpha}{2}}\right] \quad (2)$$

Where, $\Omega = \frac{\Gamma(\mu)}{\Gamma(\mu+\frac{2}{\alpha})}$ from [16]. The expression of [17, (1.125)] is given as,

$$H_{0,1}^{1,0} \left[B \left| \begin{matrix} - \\ (k, Z) \end{matrix} \right. \right] = Z^{-1} B^{\frac{k}{Z}} \exp\left(-B^{\frac{1}{Z}}\right) \quad (3)$$

Where, $H_r^r[\cdot, \cdot]$ denotes the Fox H -function and applying $B = \frac{w}{\Omega}$, $k = \mu - \frac{2}{\alpha}$ and $Z = \frac{2}{\alpha}$ in (2), it can be found that

$$f_W(w) = \frac{1}{\Omega \Gamma(\mu)} H_{0,1}^{1,0} \left[\frac{w}{\Omega} \left| \begin{matrix} - \\ \left(\mu - \frac{2}{\alpha}, \frac{2}{\alpha}\right) \end{matrix} \right. \right] \quad (4)$$

Hence, (4) can be written as,

$$f_W(w) = \varphi H_{0,1}^{1,0} \left[a w \left| \begin{matrix} - \\ \xi \end{matrix} \right. \right] \quad (5)$$

Whereby, $\varphi = \frac{1}{\Omega \Gamma(\mu)}$; $a = \frac{1}{\Omega}$; and $\xi = \left(\mu - \frac{2}{\alpha}, \frac{2}{\alpha}\right)$. The instantaneous received SNR γ at the destination or user is $\gamma = \bar{\gamma} W$, here $\bar{\gamma}$ is the average power at the receiver side. Applying RV transformation, the PDF of instantaneous SNR can be found as

$$f_\gamma(\gamma) = \frac{\varphi}{\bar{\gamma}} H_{0,1}^{1,0} \left[\frac{a}{\bar{\gamma}} \gamma \left| \begin{matrix} - \\ \xi \end{matrix} \right. \right] \quad (6)$$

3. ASER Investigation

The ASER is generally described as [20],

$$P_{ar} = \int_0^\infty Pr(e|\gamma) f_\gamma(\gamma) d\gamma \quad (7)$$

Whereby, $Pr(e|\gamma)$ Conditional Error Probability (CEP) depends on the modulation technique applied.

3.1. ASER for HQAM Subject to α - μ Fading Channels

For M-ary HQAM, the CEP is expressed as [1][12],

$$Pr_{HQAM}(e|\gamma) = A_{YY}Q(\sqrt{l\gamma}) + \frac{2}{3}A_{YY}Q^2\left(\sqrt{\frac{2l\gamma}{3}}\right) - 2A_{ZYY}Q(\sqrt{l\gamma})Q\left(\sqrt{\frac{l\gamma}{3}}\right) \quad (8)$$

Whereby, $\iota = \frac{24}{7M-4}$, $A_{YY} = 2\left(3 - \frac{4}{\sqrt{M}} + \frac{1}{M}\right)$, as well as $A_{ZYY} = 6\left(1 - \frac{1}{\sqrt{M}}\right)^2$. Prony approximation is the most accurate approximation of the Gaussian Q-function $Q(\cdot)$. Prony approximation with two exponential terms can be written as $Q(t) \approx \kappa e^{-\lambda t^2} + \delta e^{-\varepsilon t^2}$ [21]. The value of the constants is $\kappa = 0.208$, $\delta = 0.147$, $\lambda = 0.971$, and $\varepsilon = 0.525$. Putting Prony approximation in (8) produces,

$$Pr_{HQAM}(e|\gamma) = A_{YY}(\kappa e^{-\lambda l\gamma} + \delta e^{-\varepsilon l\gamma}) + \frac{2}{3}A_{YY}\left(\kappa^2 e^{-\frac{4\lambda l\gamma}{3}} + 2\kappa\delta e^{-\frac{2\lambda l\gamma}{3} - \frac{2\varepsilon l\gamma}{3}} + \delta^2 e^{-\frac{4\varepsilon l\gamma}{3}}\right) - 2A_{ZYY}(\kappa e^{-\lambda l\gamma} + \delta e^{-\varepsilon l\gamma})\left(\kappa e^{-\lambda \frac{l\gamma}{3}} + \delta e^{-\varepsilon \frac{l\gamma}{3}}\right) \quad (9)$$

Pretending (6) and (9) into (7), the ASER can be yielded as

$$P_{ar,HQAM} = A_1 + A_2 - A_3 \quad (10)$$

Where,

$$A_1 = \frac{A_{YY}\varphi}{\bar{\gamma}} \int_0^\infty (\kappa e^{-\lambda l\gamma} + \delta e^{-\varepsilon l\gamma}) H_{0,1}^{1,0} \left[\frac{a}{\bar{\gamma}} \gamma \left| \frac{-}{\xi} \right. \right] d\gamma \quad (11)$$

$$A_2 = \frac{A_{YY}2\varphi}{3\bar{\gamma}} \int_0^\infty \left(\kappa^2 e^{-\frac{4\lambda l\gamma}{3}} + 2\kappa\delta e^{-\frac{2\lambda l\gamma}{3} - \frac{2\varepsilon l\gamma}{3}} + \delta^2 e^{-\frac{4\varepsilon l\gamma}{3}} \right) \times H_{0,1}^{1,0} \left[\frac{a}{\bar{\gamma}} \gamma \left| \frac{-}{\xi} \right. \right] d\gamma \quad (12)$$

and

$$A_3 = \frac{A_{ZYY}2\varphi}{\bar{\gamma}} \times \int_0^\infty \left(\kappa^2 e^{-\gamma\left(\frac{4\lambda\iota}{3}\right)} + \kappa\delta e^{-\gamma(\lambda + \varepsilon\frac{\iota}{3})} + \kappa\delta e^{-\gamma(\varepsilon\iota + \lambda\frac{\iota}{3})} + \delta^2 e^{-\gamma\left(\frac{4\varepsilon\iota}{3}\right)} \right) H_{0,1}^{1,0} \left[\frac{a}{\bar{\gamma}} \gamma \left| \frac{-}{\xi} \right. \right] d\gamma \quad (13)$$

Putting $e^{-\omega} = H_{0,1}^{1,0} \left[\omega \left| \frac{-}{(0,1)} \right. \right]$ from [22] and solving the integration using [20, (2.25.1.1)],

$$A_1 = \frac{A_{YY}\kappa\varphi}{\lambda\bar{\gamma}} H_{1,1}^{1,1} \left[\frac{a}{\lambda\bar{\gamma}} \left| \frac{(0,1)}{\xi} \right. \right] + \frac{A_{YY}\delta\varphi}{\varepsilon\bar{\gamma}} H_{1,1}^{1,1} \left[\frac{a}{\varepsilon\bar{\gamma}} \left| \frac{(0,1)}{\xi} \right. \right] \quad (14)$$

$$A_2 = \frac{A_{YY}\kappa^2\varphi}{2\lambda\bar{\gamma}} H_{1,1}^{1,1} \left[\frac{3a}{4\lambda\bar{\gamma}} \left| \frac{(0,1)}{\xi} \right. \right] + \frac{A_{YY}2\kappa\delta\varphi}{\iota(\lambda + \varepsilon)\bar{\gamma}} H_{1,1}^{1,1} \left[\frac{3a}{2\iota(\lambda + \varepsilon)\bar{\gamma}} \left| \frac{(0,1)}{\xi} \right. \right] + \frac{A_{YY}\delta^2\varphi}{2\varepsilon\bar{\gamma}} H_{1,1}^{1,1} \left[\frac{3a}{4\varepsilon\bar{\gamma}} \left| \frac{(0,1)}{\xi} \right. \right] \quad (15)$$

and,

$$A_3 = \frac{A_{ZYY}3\kappa^2\varphi}{2\lambda\bar{\gamma}} H_{1,1}^{1,1} \left[\frac{3a}{4\lambda\bar{\gamma}} \left| \frac{(0,1)}{\xi} \right. \right] + \frac{A_{ZYY}6\kappa\delta\varphi}{\iota(3\lambda + \varepsilon)\bar{\gamma}} H_{1,1}^{1,1} \left[\frac{3a}{\iota(3\lambda + \varepsilon)\bar{\gamma}} \left| \frac{(0,1)}{\xi} \right. \right] + \frac{A_{ZYY}6\kappa\delta\varphi}{\iota(3\varepsilon + \lambda)\bar{\gamma}} H_{1,1}^{1,1} \left[\frac{3a}{\iota(3\varepsilon + \lambda)\bar{\gamma}} \left| \frac{(0,1)}{\xi} \right. \right] + \frac{A_{ZYY}3\delta^2\varphi}{2\varepsilon\bar{\gamma}} H_{1,1}^{1,1} \left[\frac{3a}{4\varepsilon\bar{\gamma}} \left| \frac{(0,1)}{\xi} \right. \right] \quad (16)$$

3.2. ASER Analysis for XQAM Subject to α - μ Fading Channels

For $L \times M$ XQAM, the $Pr(e|\gamma)$ is written as [23],

$$Pr_{XQAM}(e|\gamma) = B_{YY}Q(v\sqrt{\gamma}) - B_{ZYY}Q^2(v\sqrt{\gamma}) \quad (17)$$

Whereby $v = \sqrt{\frac{96}{31L \times M - 32}}$, $B_{YY} = 2\left(2 - \frac{1}{L} - \frac{1}{M}\right)$, and $B_{ZYY} = 4\left(1 - \frac{1}{L} - \frac{1}{M} + \frac{2}{L+M}\right)$. Inserting the Prony approximation into (17), $Pr(e|\gamma)$ is presented as

$$Pr_{XQAM}(e|\gamma) = B_{YY}(\kappa e^{-\lambda v^2\gamma} + \delta e^{-\varepsilon v^2\gamma}) - B_{ZYY}(\kappa^2 e^{-2\lambda v^2\gamma} + \delta^2 e^{-2\varepsilon v^2\gamma} + 2\kappa\delta e^{-\lambda v^2\gamma - \varepsilon v^2\gamma}) \quad (18)$$

Inserting (18) and (6) into (7), the ASER can be written as

$$P_{ar,XQAM} = \theta_1 - \theta_2. \quad (19)$$

Whereby,

$$\theta_1 = \frac{B_{YY}\varphi}{\bar{\gamma}} \int_0^\infty (\kappa e^{-\lambda v^2\gamma} + \delta e^{-\varepsilon v^2\gamma}) H_{0,1}^{1,0} \left[\frac{a}{\bar{\gamma}} \gamma \left| \frac{-}{\xi} \right. \right] d\gamma \quad (20)$$

and,

$$\theta_2 = \frac{B_{ZYY}\varphi}{\bar{\gamma}} \int_0^\infty \left(\kappa^2 e^{-2\lambda v^2\gamma} + 2\kappa\delta e^{-\lambda v^2\gamma - \varepsilon v^2\gamma} + \delta^2 e^{-2\varepsilon v^2\gamma} \right) H_{0,1}^{1,0} \left[\frac{a}{\bar{\gamma}} \gamma \left| \frac{-}{\xi} \right. \right] d\gamma \quad (21)$$

Replacing the exponential terms with Fox H -function and solving the integration using [20, (2.25.1.1)],

$$\begin{aligned} \Theta_1 &= \frac{B_{YY}\kappa\varphi}{\lambda v^2 \bar{\gamma}} H_{1,1}^{1,1} \left[\frac{a}{\lambda v^2 \bar{\gamma}} \middle| \begin{matrix} (0,1) \\ \xi \end{matrix} \right] \\ &+ \frac{B_{YY}\delta\varphi}{\varepsilon v^2 \bar{\gamma}} H_{1,1}^{1,1} \left[\frac{a}{\varepsilon v^2 \bar{\gamma}} \middle| \begin{matrix} (0,1) \\ \xi \end{matrix} \right] \end{aligned} \quad (22)$$

and,

$$\begin{aligned} \Theta_2 &= \frac{B_{ZYY}\kappa^2\varphi}{2\lambda v^2 \bar{\gamma}} H_{1,1}^{1,1} \left[\frac{a}{2\lambda v^2 \bar{\gamma}} \middle| \begin{matrix} (0,1) \\ \xi \end{matrix} \right] \\ &+ \frac{B_{ZYY}2\kappa\delta\varphi}{(\lambda+\varepsilon)v^2 \bar{\gamma}} H_{1,1}^{1,1} \left[\frac{a}{(\lambda+\varepsilon)v^2 \bar{\gamma}} \middle| \begin{matrix} (0,1) \\ \xi \end{matrix} \right] \\ &+ \frac{B_{ZYY}\delta^2\varphi}{2\varepsilon v^2 \bar{\gamma}} H_{1,1}^{1,1} \left[\frac{a}{2\varepsilon v^2 \bar{\gamma}} \middle| \begin{matrix} (0,1) \\ \xi \end{matrix} \right] \end{aligned} \quad (23)$$

3.3. ASER Analysis for SQAM Subject to α - μ Fading Channels

For M -ary SQAM, the $Pr(e|\gamma)$ can be expressed as [23],

$$Pr_{SQAM}(e|\gamma) = C_{YY}Q(\rho\sqrt{\gamma}) - C_{ZYY}Q^2(\rho\sqrt{\gamma}) \quad (24)$$

Where $\rho = \sqrt{\frac{3}{M-1}}$, $C_{YY} = 4\left(1 - \frac{1}{\sqrt{M}}\right)$, and $C_{ZYY} = 4\left(1 - \frac{1}{\sqrt{M}}\right)^2$. Replacing $Q(\cdot)$ with the Prony approximation,

$$\begin{aligned} Pr_{SQAM}(e|\gamma) &= C_{YY}(\kappa e^{-\lambda\rho^2\gamma} + \delta e^{-\varepsilon\rho^2\gamma}) \\ &- C_{ZYY}(\kappa^2 e^{-2\lambda\rho^2\gamma} + \delta^2 e^{-2\varepsilon\rho^2\gamma} + 2\kappa\delta e^{-\lambda\rho^2\gamma - \varepsilon\rho^2\gamma}) \end{aligned} \quad (25)$$

Substituting (25) and (6) into (7), the ASER can be written as

$$P_{ar,SQAM} = \Omega_1 - \Omega_2 \quad (26)$$

Where,

$$\Omega_1 = \frac{C_{YY}\varphi}{\bar{\gamma}} \int_0^\infty (\kappa e^{-\lambda\rho^2\gamma} + \delta e^{-\varepsilon\rho^2\gamma}) H_{0,1}^{1,0} \left[\frac{a}{\bar{\gamma}} \gamma \middle| \begin{matrix} - \\ \xi \end{matrix} \right] d\gamma \quad (27)$$

and,

$$\begin{aligned} \Omega_2 &= \frac{C_{ZYY}\varphi}{\bar{\gamma}} \int_0^\infty (\kappa^2 e^{-2\lambda\rho^2\gamma} + 2\kappa\delta e^{-\lambda\rho^2\gamma - \varepsilon\rho^2\gamma} \\ &+ \delta^2 e^{-2\varepsilon\rho^2\gamma}) H_{0,1}^{1,0} \left[\frac{a}{\bar{\gamma}} \gamma \middle| \begin{matrix} - \\ \xi \end{matrix} \right] d\gamma \end{aligned} \quad (28)$$

Expressing the exponential terms with Fox H -function and solving the integrals with the application of [20, (2.25.1.1)],

$$\begin{aligned} \Omega_1 &= \frac{C_{YY}\kappa\varphi}{\lambda\rho^2 \bar{\gamma}} H_{1,1}^{1,1} \left[\frac{a}{\lambda\rho^2 \bar{\gamma}} \middle| \begin{matrix} (0,1) \\ \xi \end{matrix} \right] \\ &+ \frac{C_{YY}\delta\varphi}{\varepsilon\rho^2 \bar{\gamma}} H_{1,1}^{1,1} \left[\frac{a}{\varepsilon\rho^2 \bar{\gamma}} \middle| \begin{matrix} (0,1) \\ \xi \end{matrix} \right] \end{aligned} \quad (29)$$

and,

$$\begin{aligned} \Omega_2 &= \frac{C_{ZYY}\kappa^2\varphi}{2\lambda\rho^2 \bar{\gamma}} H_{1,1}^{1,1} \left[\frac{a}{2\lambda\rho^2 \bar{\gamma}} \middle| \begin{matrix} (0,1) \\ \xi \end{matrix} \right] \\ &+ \frac{C_{ZYY}2\kappa\delta\varphi}{(\lambda\rho^2 + \varepsilon\rho^2) \bar{\gamma}} H_{1,1}^{1,1} \left[\frac{a}{(\lambda\rho^2 + \varepsilon\rho^2) \bar{\gamma}} \middle| \begin{matrix} (0,1) \\ \xi \end{matrix} \right] \\ &+ \frac{C_{ZYY}\delta^2\varphi}{2\varepsilon\rho^2 \bar{\gamma}} H_{1,1}^{1,1} \left[\frac{a}{2\varepsilon\rho^2 \bar{\gamma}} \middle| \begin{matrix} (0,1) \\ \xi \end{matrix} \right] \end{aligned} \quad (30)$$

3.4. ASER Analysis for RQAM Subject to α - μ Fading Channels

For $L \times M$ RQAM, the $Pr(e|\gamma)$ can be given as [22],

$$\begin{aligned} Pr_{RQAM}(e|\gamma) &= 2D_{YY}Q(q\sqrt{\gamma}) + 2D_{ZYY}Q(r\sqrt{\gamma}) \\ &- 4D_{YY}D_{ZYY}Q(q\sqrt{\gamma})Q(r\sqrt{\gamma}) \end{aligned} \quad (31)$$

Where, $D_{YY} = 1 - \frac{1}{L}$; $D_{ZYY} = 1 - \frac{1}{M}$; $q = \sqrt{\frac{6}{(L^2-1)+(M^2-1)b^2}}$; $r = bq$; the quadrature to-in-phase decision distance ratio $b = \frac{d_Q}{d_I}$. Here d_I and d_Q are in-phase as well as quadrature decision distance, respectively. Again applying the Prony approximation in (31), $Pr(e|\gamma)$ is arranged as

$$\begin{aligned} Pr_{RQAM}(e|\gamma) &= 2D_{YY}(\kappa e^{-\lambda q^2\gamma} + \delta e^{-\varepsilon q^2\gamma}) \\ &+ 2D_{ZYY}(\kappa e^{-\lambda r^2\gamma} + \delta e^{-\varepsilon r^2\gamma}) \\ &- 4D_{YY}D_{ZYY}(\kappa^2 e^{-\lambda q^2\gamma - \lambda r^2\gamma} + \kappa\delta e^{-\lambda q^2\gamma - \varepsilon r^2\gamma} \\ &+ \kappa\delta e^{-\varepsilon q^2\gamma - \lambda r^2\gamma} + \delta^2 e^{-\varepsilon q^2\gamma - \varepsilon r^2\gamma}) \end{aligned} \quad (32)$$

Putting (32) and (6) into (7), the ASER can be obtained as

$$P_{ar,RQAM} = \Phi_1 + \Phi_2 - \Phi_3. \quad (33)$$

Where,

$$\Phi_1 = \frac{D_{YY}2\varphi}{\bar{\gamma}} \int_0^\infty (\kappa e^{-\lambda q^2\gamma} + \delta e^{-\varepsilon q^2\gamma}) H_{0,1}^{1,0} \left[\frac{a}{\bar{\gamma}} \gamma \middle| \begin{matrix} - \\ \xi \end{matrix} \right] d\gamma \quad (34)$$

$$\Phi_2 = \frac{D_{ZYY}2\varphi}{\bar{\gamma}} \int_0^\infty (\kappa e^{-\lambda r^2\gamma} + \delta e^{-\varepsilon r^2\gamma}) H_{0,1}^{1,0} \left[\frac{a}{\bar{\gamma}} \gamma \middle| \begin{matrix} - \\ \xi \end{matrix} \right] d\gamma \quad (35)$$

and,

$$\Phi_3 = \frac{D_{YY}D_{ZYY}4\varphi}{\bar{\gamma}} \int_0^\infty (\kappa^2 e^{-\lambda q^2 \gamma - \lambda r^2 \gamma} + \kappa \delta e^{-\lambda q^2 \gamma - \epsilon r^2 \gamma} + \kappa \delta e^{-\epsilon q^2 \gamma - \lambda r^2 \gamma} + \delta^2 e^{-\epsilon q^2 \gamma - \epsilon r^2 \gamma}) H_{0,1}^{1,0} \left[\frac{a}{\bar{\gamma}} \gamma \middle| \xi \right] d\gamma \quad (36)$$

Writing the exponential terms with Fox H -function and simplifying the integrals employing [20, (2.25.1.1)],

$$\Phi_1 = \frac{D_{YY}2\kappa\varphi}{\lambda q^2 \bar{\gamma}} H_{1,1}^{1,1} \left[\frac{a}{\lambda q^2 \bar{\gamma}} \middle| \xi \right] (0,1) + \frac{D_{YY}2\delta\varphi}{\epsilon q^2 \bar{\gamma}} H_{1,1}^{1,1} \left[\frac{a}{\epsilon q^2 \bar{\gamma}} \middle| \xi \right] (0,1) \quad (37)$$

$$\Phi_2 = \frac{D_{ZYY}2\kappa\varphi}{\lambda r^2 \bar{\gamma}} H_{1,1}^{1,1} \left[\frac{a}{\lambda r^2 \bar{\gamma}} \middle| \xi \right] (0,1) + \frac{D_{ZYY}2\delta\varphi}{\epsilon r^2 \bar{\gamma}} H_{1,1}^{1,1} \left[\frac{a}{\epsilon r^2 \bar{\gamma}} \middle| \xi \right] (0,1) \quad (38)$$

and,

$$\Phi_3 = \frac{D_{YY}D_{ZYY}4\kappa^2\varphi}{(q^2 + r^2)\lambda\bar{\gamma}} H_{1,1}^{1,1} \left[\frac{a}{(q^2 + r^2)\lambda\bar{\gamma}} \middle| \xi \right] (0,1) + \frac{D_{YY}D_{ZYY}4\kappa\delta\varphi}{(\lambda q^2 + \epsilon r^2)\bar{\gamma}} H_{1,1}^{1,1} \left[\frac{a}{(\lambda q^2 + \epsilon r^2)\bar{\gamma}} \middle| \xi \right] (0,1) + \frac{D_{YY}D_{ZYY}4\kappa\delta\varphi}{(\epsilon q^2 + \lambda r^2)\bar{\gamma}} H_{1,1}^{1,1} \left[\frac{a}{(\epsilon q^2 + \lambda r^2)\bar{\gamma}} \middle| \xi \right] (0,1) + \frac{D_{YY}D_{ZYY}4\delta^2\varphi}{(q^2 + r^2)\epsilon\bar{\gamma}} H_{1,1}^{1,1} \left[\frac{a}{(q^2 + r^2)\epsilon\bar{\gamma}} \middle| \xi \right] (0,1) \quad (39)$$

4. Analytical Consequences and Analysis

The numerical derivations of the previous section are evaluated and plotted for analysis. Figure 1 shows the ASER vs average SNR curves for 8-HQAM and 16-HQAM techniques while considering the different channel fading parameters α and μ values. It can be acquired that ASER performance deteriorates with 16-HQAM as compared to 8-HQAM, which is because the large constellation size is more affected by channel fading.

It is reflected that the ASER performance becomes weak with $\alpha=1$, $\mu=1$ (Exponential distribution) as correlated to $\alpha=2$, $\mu=1$ (Rayleigh distribution). The ASER performance improves with $\alpha=2$, $\mu=2$ (Nakagami- m distribution with $m=2$). The ASER performance becomes better with the increase in the amount of fading parameter μ and for a constant value of α , signifying that the increase in multipath clusters in the channel results in less fading effect. In

addition, by increasing the value of α and keeping μ constant, the ASER performance enhances, referring that the increase in nonlinearity turns the channel conditions into a better position.

In Figure 2, ASER vs average SNR has been illustrated for 8x4 XQAM techniques subject to different values of α and μ . It is found that ASER performance is better with 8x4 XQAM than XQAM with a large number of symbols since small constellation size is less affected by channel fading. The ASER performance is better with $\alpha=2$, $\mu=2$ (Nakagami- m distribution for $m=2$) as compared to $\alpha=2$, $\mu=1$ (Rayleigh distribution).

The ASER performance deteriorates with $\alpha=1$, $\mu=1$ (Exponential fading distribution). Moreover, the ASER performance boosts with the addition of fading parameter μ and for a fixed value of α , signifying the addition in the number of multipath clusters improves the channel situation. Similarly, by increasing α for a fixed value of μ , the ASER reduces because the increase in nonlinearity indicates the influence of minor fading.

In Figure 3, ASER vs average SNR has been depicted for the 16-SQAM technique by varying the values of α and μ . ASER performance improves with 4-SQAM compared to 16-SQAM since the small constellation size may improve the fading effect. The ASER increases while the amount of nonlinearity parameter α decreases for a particular value of μ . This is because the lower the amount of α , the more the fading issue. Likewise, ASER deteriorates while the multipath clusters parameter μ decreases for a particular value of α because of poor channel condition.

In Figure 4, ASER vs Average SNR has been depicted for 4x2 RQAM and 4x4 RQAM over different values of α and μ . Here decision distance ratio is considered as $b=1$. ASER value is much less for 4x2 RQAM than for 4x4 RQAM. Large constellation size suffers more fading effects. ASER performance improves with an increase in α due to less fading effect. ASER performance improves with an increase in μ due to good channel condition.

Figure 5 shows the ASER plots considering the transmission of 16 symbols for HQAM, SQAM and RQAM schemes with $\alpha=1$ and $\mu=1$. ASER reduces with SQAM and RQAM compared to the HQAM scheme. The analysis shows that ASER performance improves with XQAM compared to HQAM since the XQAM technique has less peak and average signal power. The energy-efficient Two-Dimensional (2D) structure of XQAM is more suitable than SQAM, and the odd power of 2 constellations is RQAM.

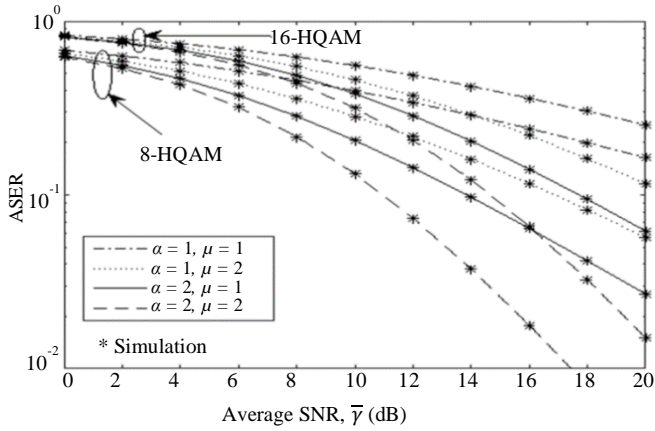


Fig. 1 ASER vs Average SNR (dB) using HQAM for different α and μ

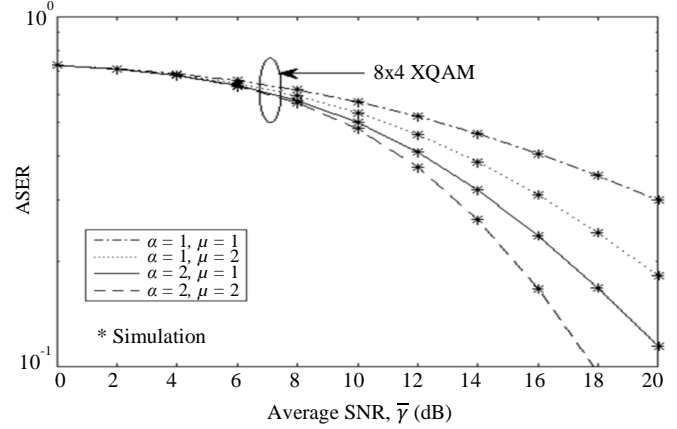


Fig. 2 ASER vs Average SNR (dB) using XQAM for different α and μ

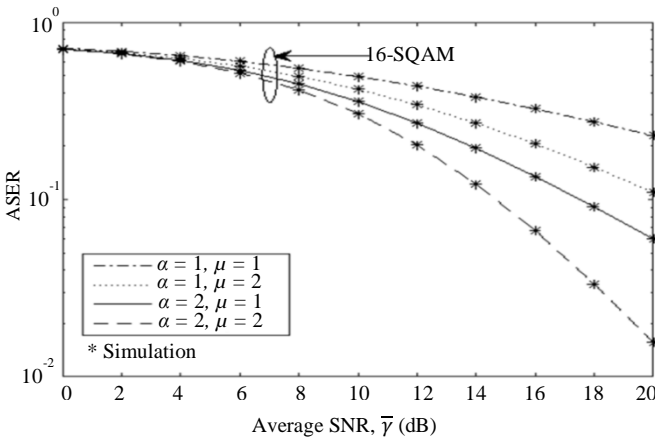


Fig. 3 ASER vs Average SNR (dB) using SQAM for different α and μ

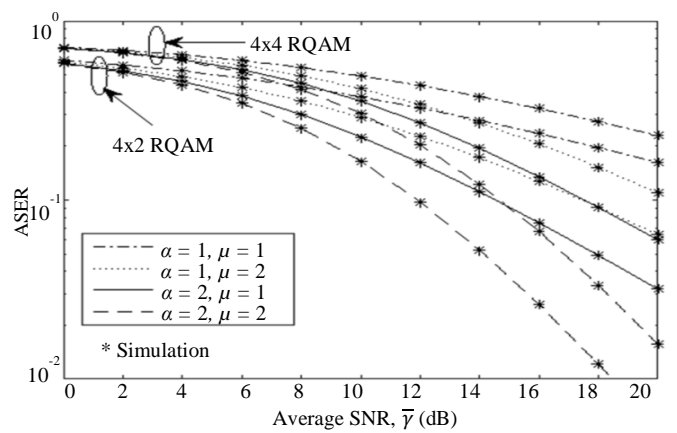


Fig. 4 ASER vs Average SNR (dB) using RQAM for different α and μ

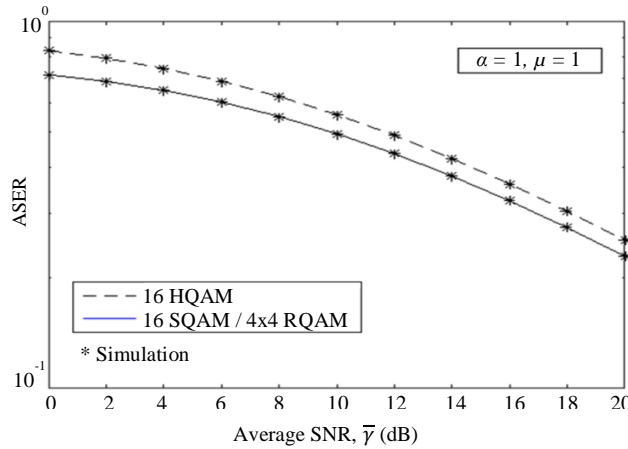


Fig. 5 Comparison of ASER vs Average SNR (dB) utilizing different QAM techniques and for $\alpha=1, \mu=1$

5. Conclusion

The ASER of the SISO communication system subject to α - μ fading channels is analyzed in this article. Different QAM techniques like HQAM, XQAM, SQAM and RQAM are applied to observe the ASER performance. The Prony approximation, which is the most accurate one, is utilized for Gaussian Q -function. The expressions of ASER are derived

concerning the Fox H -function, the most useful function. The arbitrary value of the nonlinearity parameter and multipath cluster parameter are considered for the analysis.

The arbitrary number of constellation sizes for different QAM techniques is utilized to investigate the ASER. Using the small constellation pattern outcomes a better ASER

performance since fewer symbols are affected by the operating environment. Again when the channel is influenced by less fading, i.e. for the high nonlinearity parameter, the ASER performance improves. The ASER performance

improves for the immense value of the multipath clusters environment. Lastly, computer-simulated data have been utilized to determine the accuracy of the derived numerical statements.

References

- [1] Luca Rugini, "Symbol Error Probability of Hexagonal QAM," *IEEE Communications Letters*, vol. 20, no. 8, pp. 1523-1526, 2016. [[CrossRef](#)] [[Google Scholar](#)] [[Publisher Link](#)]
- [2] Nagendra Kumar, Praveen Kumar Singya, and Vimal Bhatia, "ASER Analysis of Hexagonal and Rectangular QAM Schemes in Multiple-Relay Networks," *IEEE Transactions on Vehicular Technology*, vol. 67, no. 2, pp. 1815-1819, 2018. [[CrossRef](#)] [[Google Scholar](#)] [[Publisher Link](#)]
- [3] Xi-chun Zhang, Hua Yu, and Gang Wei, "Exact Symbol Error Probability of Cross-QAM in AWGN and Fading Channels," *EURASIP Journal on Wireless Communications and Networking*, vol. 2010, pp. 1-9, 2010. [[CrossRef](#)] [[Google Scholar](#)] [[Publisher Link](#)]
- [4] Praveen Kumar Singya et al., "A Survey on Higher-Order QAM Constellations: Technical Challenges, Recent Advances, and Future Trends," *IEEE Open Journal of the Communications Society*, vol. 2, pp. 617-655, 2021. [[CrossRef](#)] [[Google Scholar](#)] [[Publisher Link](#)]
- [5] Marvin K. Simon, and Mohamed-Slim Alouini, *Digital Communication over Fading Channels*, A Wiley-Interscience Publication, 2005. [[Google Scholar](#)] [[Publisher Link](#)]
- [6] Dharmendra Dixit, and P. R. Sahu, "Performance Analysis of Rectangular QAM with SC Receiver over Nakagami- m Fading Channels," *IEEE Communications Letters*, vol. 18, no. 7, pp. 1262-1265, 2014. [[CrossRef](#)] [[Google Scholar](#)] [[Publisher Link](#)]
- [7] Michel Daoud Yacoub, "The α - μ Distribution: A Physical Fading Model for the Stacy Distribution," *IEEE Transactions on Vehicular Technology*, vol. 56, no. 1, pp. 27-34, 2007. [[CrossRef](#)] [[Google Scholar](#)] [[Publisher Link](#)]
- [8] Hua Yu et al., "On the Error Probability of Cross-QAM with MRC Reception over Generalized η - μ Fading Channels," *IEEE Transactions on Vehicular Technology*, vol. 60, no. 6, pp. 2631-2643, 2011. [[CrossRef](#)] [[Google Scholar](#)] [[Publisher Link](#)]
- [9] Dharmendra Dixit, and P. R. Sahu, "Performance of QAM Signaling over TWDP Fading Channels," *IEEE Transactions on Wireless Communications*, vol. 12, no. 4, pp. 1794-1799, 2013. [[CrossRef](#)] [[Google Scholar](#)] [[Publisher Link](#)]
- [10] Kanchan K. Masade, and D. M. Bhalerao, "Fifth Generation of Mobile Wireless Communication: 5G," *International Journal of P2P Network Trends and Technology (IJPTT)*, vol. 7, no. 3, pp. 1-5, 2017. [[CrossRef](#)] [[Publisher Link](#)]
- [11] Taimour Aldalgamouni et al., "Performance Analysis of Fisher-Snedecor F Composite Fading Channels," *2018 IEEE Middle East and North Africa Communications Conference (MENACOMM)*, Lebanon, pp. 1-5, 2018. [[CrossRef](#)] [[Google Scholar](#)] [[Publisher Link](#)]
- [12] Mehmet Bilim, "Different QAM Schemes Analyses for ARS Fading Channels," *Transactions on Emerging Telecommunications Technologies*, vol. 32, no. 1, p. e4119, 2020. [[CrossRef](#)] [[Google Scholar](#)] [[Publisher Link](#)]
- [13] Mehmet Bilim, "Dual-Branch SC Wireless Systems with HQAM for Beyond 5G over η - μ Fading Channels," *Peer-to-Peer Networking and Applications*, vol. 14, pp. 305-318, 2021. [[CrossRef](#)] [[Google Scholar](#)] [[Publisher Link](#)]
- [14] Thrassos K. Oikonomou et al., "On the Error Analysis of Hexagonal-QAM Constellations," *IEEE Communications Letters*, vol. 26, no. 8, pp. 1764-1768, 2022. [[CrossRef](#)] [[Google Scholar](#)] [[Publisher Link](#)]
- [15] Diogo Matos et al., "On the Performance of Square, Rectangular, Star, and Hexagonal QAM for Backscatter Systems," *IEEE Microwave and Wireless Technology Letters*, vol. 33, no. 1, pp. 102-105, 2023. [[CrossRef](#)] [[Google Scholar](#)] [[Publisher Link](#)]
- [16] Satoshi Kodama, and Sari Nagao, "Application of Existing Network Methods in Low Power Long Range Wireless Communication," *International Journal of P2P Network Trends and Technology*, vol. 10, no. 1, pp. 1-9, 2020. [[CrossRef](#)] [[Google Scholar](#)] [[Publisher Link](#)]
- [17] L. Kong, H. Tran, and G. Kaddoum, "Performance Analysis of Physical Layer Security over α - μ Fading Channel," *Electronics Letters*, vol. 52, no. 1, pp. 45-47, 2016. [[CrossRef](#)] [[Google Scholar](#)] [[Publisher Link](#)]
- [18] A. M. Mathai, R. K. Saxena, and H. J. Haubold, *The H-Function: Theory and Applications*, Springer Science and Business Media, 2009. [[CrossRef](#)] [[Google Scholar](#)] [[Publisher Link](#)]
- [19] J. G. Proakis, *Digital Communications*, McGraw-Hill, 2001. [[Google Scholar](#)]
- [20] Pavel Loskot, and Norman C. Beaulieu, "Prony and Polynomial Approximations for Evaluation of the Average Probability of Error over Slow-Fading Channels," *IEEE Transactions on Vehicular Technology*, vol. 58, no. 3, pp. 1269-1280, 2009. [[CrossRef](#)] [[Google Scholar](#)] [[Publisher Link](#)]
- [21] Anatolii Platonovich Prudnikov et al., *Integrals and Series: More Special Functions*, Gordon and Breach Science Publishers, 1990. [[Google Scholar](#)]
- [22] Dharmendra Sadhwani, "Simple and Tightly Approximated Integrals over κ - μ Shadowed Fading Channel with Applications," *IEEE Transactions on Vehicular Technology*, vol. 67, no. 10, pp. 10092-10096, 2018. [[CrossRef](#)] [[Google Scholar](#)] [[Publisher Link](#)]
- [23] N. C. Beaulieu, "A Useful Integral for Wireless Communication Theory and Its Application to Rectangular Signaling Constellation Error Rates," *IEEE Transactions on Communications*, vol. 54, no. 5, pp. 802-805, 2006. [[CrossRef](#)] [[Google Scholar](#)] [[Publisher Link](#)]